JOM, Vol. 68, No. 10, 2016
DOI: 10.1007/s11837-016-1953-7

Effect of Samarium Oxide on the Electrical Conductivity of Plasma-Sprayed SOFC Anodes

S.N. PANAHI,[1] H. SAMADI,[2,4] and A. NEMATI[3]

1.—Department of Materials Engineering, Science and Research Branch, Islamic Azad University, Tehran, Iran. 2.—Department of Materials Science and Engineering, Faculty of Engineering, Malayer University, Malayer, Iran. 3.—Department of Materials Science and Engineering, Sharif University of Technology, Tehran, Iran. 4.—e-mail: hamed.samadi@utoronto.ca

Solid oxide fuel cells (SOFCs) are rapidly becoming recognized as a new alternative to traditional energy conversion systems because of their high energy efficiency. From an ecological perspective, this environmentally friendly technology, which produces clean energy, is likely to be implemented more frequently in the future. However, the current SOFC technology still cannot meet the demands of commercial applications due to temperature constraints and high cost. To develop a marketable SOFC, suppliers have tended to reduce the operating temperatures by a few hundred degrees. The overall trend for SOFC materials is to reduce their service temperature of electrolyte. Meanwhile, it is important that the other components perform at the same temperature. Currently, the anodes of SOFCs are being studied in depth. Research has indicated that anodes based on a perovskite structure are a more promising candidate in SOFCs than the traditional system because they possess more favorable electrical properties. Among the perovskite-type oxides, $SrTiO_3$ is one of the most promising compositions, with studies demonstrating that $SrTiO_3$ exhibits particularly favorable electrical properties in contrast with other perovskite-type oxides. The main purpose of this article is to describe our study of the effect of rare-earth dopants with a perovskite structure on the electrical behavior of anodes in SOFCs. Sm_2O_3-doped $SrTiO_3$ synthesized by a solid-state reaction was coated on substrate by atmospheric plasma spray. To compare the effect of the dopant on the electrical conductivity of strontium titanate, different concentrations of Sm_2O_3 were used. The samples were then investigated by x-ray diffraction, four-point probe at various temperatures (to determine the electrical conductivity), and a scanning electron microscope. The study showed that at room temperature, nondoped samples have a higher electrical resistance than doped samples. As the temperature was increased, the electrical conductivity correspondingly increased. The optimum value of 1.1 S/cm was found at 340°C for samples with 1.5% mol Sm_2O_3.

INTRODUCTION

Worldwide energy demand has been continually increasing. The current hydrocarbon fuels, such as oil, coal, and natural gas (the world's main sources of energy), carry two major problems. First, they are limited; and second, they have been criticized for causing global warming as a result of the associated carbon dioxide emissions.[1]

Solid oxide fuel cells (SOFCs) are one of the most realistic candidates for a new generation power system because they possess high-energy conversion efficiency and environmental compatibility, promote rapid reaction kinetics, and allow for internal reforming of hydrocarbon fuels or direct oxidation at the surface of the anode electrode. These characteristics make SOFCs potentially more competitive than the present power generation

(Published online May 25, 2016)

systems.[2–4] Currently, the major obstacle to commercializing SOFCs is the high cost associated with maintaining the high operating temperature (800–1000°C) that is required.

To realize commercial SOFC applications, it is necessary to reduce their cost and improve their long-term stability. One effective way to lower the cost would be to reduce the operating temperature from the very high current temperature of about 1000°C to a temperature within the intermediate range (600–800°C). This would allow lower cost interconnecting materials, which require temperatures within the intermediate range, to be used. In addition, the coarsening of porous electrodes can be considerably delayed by decreasing the temperature, consequently improving long-term durability.[5,6]

Anodes are one of the most important components of SOFCs, and since they directly face the fuel, which enters from the anode side, their durability is crucial for achieving high performance.[7,8] Unfortunately, anodes in SOFCs are easily poisoned by impurities in gas streams, such as sulfur, which is commonly present in natural gas. Hydrogen sulfide (H_2S) is the most common impurity in diesel and natural gas fuels and is recognized as a problem when operating SOFCs with conventional anodes. An example is $Ni/Y_2O_3–ZrO_2$ (Ni/YSZ), which is rapidly poisoned by H_2S, causing it to lose its capacity for electrochemical oxidation of hydrogen. Thus, there is a huge demand for nickel-free anodes in the SOFC world to reduce the weight, cost, resistivity, and the dissipation of energy. All the aforementioned major factors point individually in the same direction—development of "novel anodes," from the materials' point of view, operating at intermediate temperatures of 500–800°C or less.[7,9–11] Perovskite-like materials with electronic or mixed ionic-electronic conductivity make the triple-phase boundary (TPB) extend to the entirely exposed anode surface and are considered a possible substitute to nickel in SOFC anodes. Among perovskite-like materials, $SrTiO_3$ is one of the most promising compositions because it can accommodate various dopants and incorporate cations with multiple oxidation states, which provides a mechanism for higher electronic and ionic conductivity.[3,12] It also exhibits moderate thermal expansion, does not catalyze carbon deposition, and is tolerant with respect to H_2S, but in a pure form, it is a dielectric material. The source of increased electronic conductivity upon doping with Sm_2O_3 can be explained by the fact that $SrTiO_3$'s A and B sites are occupied by divalent Sr^{2+} and tetravalent Ti^{4+}. Many studies are being focused on the effect of doping elements (*n*-type and *p*-type) on total conductivity of doped $SrTiO_3$ due to their unusually high electrical conductivity.[3]

Donor-doped $SrTiO_3$ ceramics are known to exhibit phase stability under both oxidizing and reducing conditions. In addition, donor doping on the Sr site of $SrTiO_3$ with a perovskite-structure dopant could improve the electrical conductivity.[3,11,13,14] Sm is a preferred choice as it can substitute Sr and perform as an *n*-type semiconductor.

SOFC components can be fabricated via methods such as tape casting, solid-state sintering, electrochemical vapor deposition (EVD), chemical vapor deposition (CVD), physical vapor deposition (PVD), and thermal spray processes. Atmospheric plasma spraying (APS), a form of thermal spraying technology, has been identified as a potential cost-reducing manufacturing technique for the porous SOFC electrodes because it has been proven to produce a full cell in minutes, and it facilitates the use of relatively inexpensive ferritic stainless steel supporting structures.[15–17]

The aim of this study was to investigate the effect of rare-earth *n*-type dopants (Sm) on Sr site on the electrical conductivity of anodes in SOFCs.

EXPERIMENTAL APPROACH

The $Sr_{1-x}Sm_xTiO_3$ (SST) (x = 0, 0.015, and 0.035) samples were prepared by the solid-state reaction method. Starting powders of $SrCO_3$ (Sigma-Aldrich, Germany), TiO_2, and Sm_2O_3 (Merck, Germany) in a stochiometric proportion were thoroughly mixed using a planetary ball mill at 200 rpm for 1 h. Then, the processed powders were sintered at 1450°C for 1.5 h. The coatings were sprayed using a 3-MB air plasma spray gun (Sulzer, IN, USA). The spraying conditions are listed in Table I.

The phase formation was investigated via x-ray diffraction (XRD), (PW1800, PHILIPS, The Netherlands), with the electrical conductivity of the samples at room temperature being measured by four-point probe (Keithley, 196 Sys DMM, 2, USA) and a setup established for high temperatures.

RESULTS AND DISCUSSION

X-ray Diffraction

Figure 1 shows the XRD patterns of the synthesized powders. As shown in Fig. 1a, the $SrTiO_3$ sample has a single phase according to JCPDS file 73-661. While in both Fig. 1b and c, peaks of Sm_2O_3 were detected in the Sm-doped samples. However,

Table I. Plasma spray parameters

Operating power	22.5 kW
Voltage	50 V
Current	450 A
Primary gas (Ar) flow rate	10 L/min
Secondary gas (H_2) flow rate	5 L/min
Carrier gas (Ar) pressure	275 kPa
Powder feed rate	20 g/min
Spray distance	100 mm

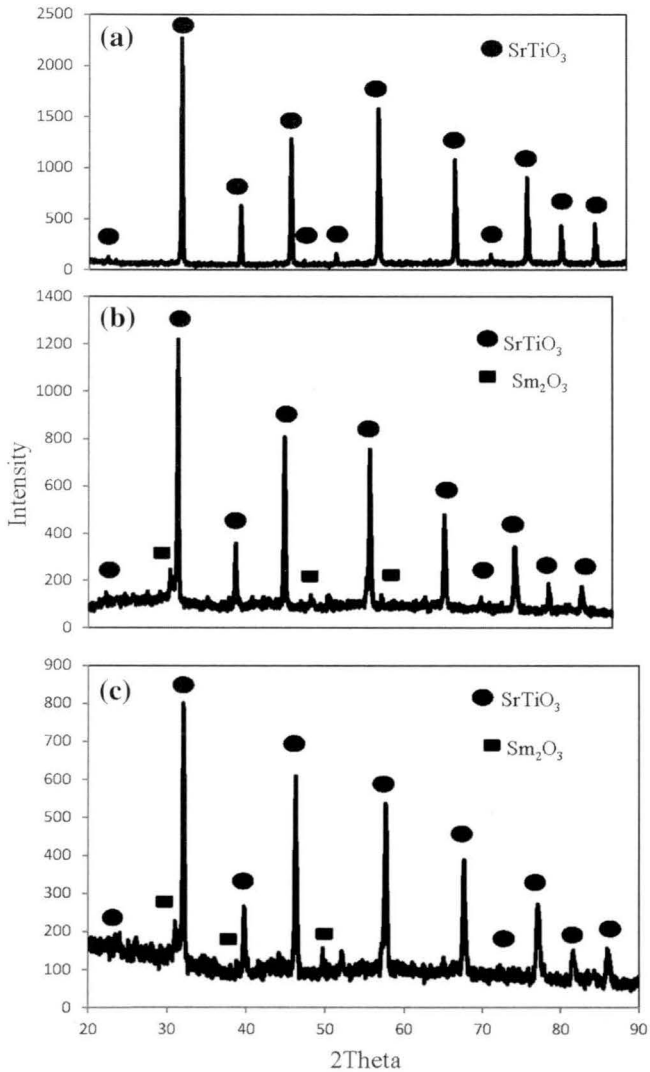

Fig. 1. XRD patterns of $Sr_{1-x}Sm_xTiO_3$ samples with different amounts of Sm_2O_3: (a) not dopped $SrTiO_3$, (b) $SrTiO_3$ dopped with 1.5% mol Sm_2O_3, and (c) $SrTiO_3$ dopped with 3.5% mol Sm_2O_3.

these impurity peaks were quite small, which indicates that almost all of the raw materials fully reacted during the synthesis.[18]

The average crystallite size was estimated using Scherrer's formula:

$$D = \frac{0.9\lambda}{\beta \cos \theta} \quad (1)$$

where D is the average crystallite size in nanometers, λ is the wavelength of the radiation, β is the peak width at half-maximum intensity, and θ is the peak position.[19] The values of average crystallite size are listed in Table II and show that the crystallites of the samples are in nano scale.

Table II. Average crystallite size of SST

x	Average crystallite size (nm)
0	44
0.015	41
0.035	33

Table III. Electrical conductivity of $Sr_{1-x}Sm_xTiO_3$ samples at room temperature

$Sr_{1-x}Sm_xTiO_3$	Sample code	σ(s/cm)
$x = 0$	SST	1.24×10^{-8}
$x = 0.015$	SST15	173×10^{-5}
$x = 0.035$	SST35	232×10^{-5}

Electrical Conductivity Measurement

Four-probe DC conductivity results at room temperature are shown in Table III for the SST samples. As demonstrated, adding Sm increases the electrical conductivity of strontium titanate dramatically.

For the doped $Sr_{1-x}Sm_xTiO_3$, the substitution of Sm for Sr resulted in an excess electron due to the different valence states of Sm^{3+} and Sr^{2+}, and because this electron was excited, $Sr_{1-x}Sm_xTiO_3$ became an n-type conductor, thus, leading to an increase of electrical conductivity with the addition of Sm content to the SST.[20]

Temperature dependence of electrical conductivity of SST, SST15, and SST35 in air is presented in Fig. 2. The conductivity in all cases increases with increasing temperature, confirming semiconducting behavior. The conductivity of all samples reached a maximum value of 1.1 S/cm at 340°C, 535°C, and 570°C for SST35, SST15, and SST, respectively, and then was almost constant up to 800°C.

As mentioned, because of commercial concerns and issues such as thermal mismatch among cell components, chemical instability, and selection of materials,[21] decreasing the working temperature of SOFCs is critical, and because novel electrolytes such as samaria-doped ceria (SDC)[22] and gadolinium-doped ceria (GDC)[21] perform at lower temperatures, other components of SOFCs, including anodes, must be produced from materials that have the ability to perform optimally at lower temperatures, as well. However, these substitutes show relatively low electrical conductivity in air due to the lack of either electronic charge carriers (Ti'_{Ti}) or ionic charge carriers ($V_O^{\cdot}$).[23] Kroger–Vink notation for doped samples is described in Eq. 2:

$$Sm_2O_3 \xrightarrow{2SrTiO_3} 2Sm_{Sr}^{\circ} + 3O_O^{\times} + V_{Sr}'' \quad (2)$$

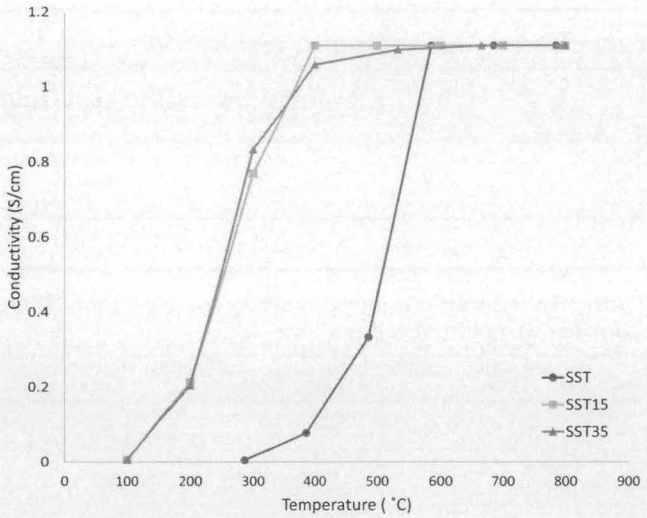

Fig. 2. Electrical conductivity of $Sr_{1-x}Sm_xTiO_3$ (x = 0, 0.015, and 0.035) measured in air.

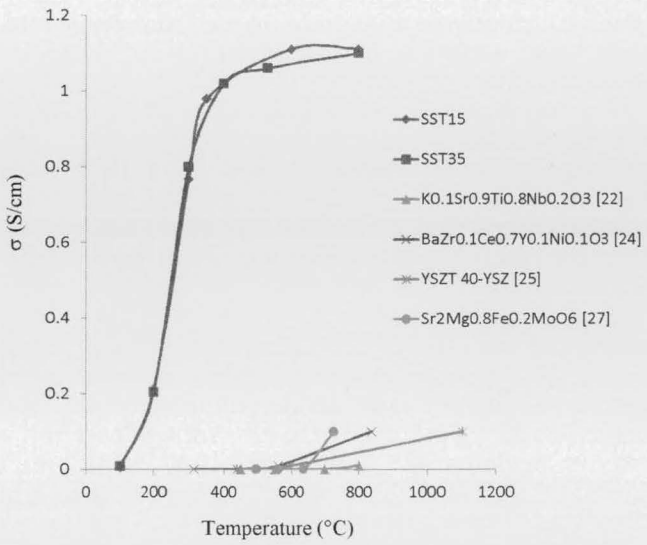

Fig. 3. Electrical conductivity comparison between different kinds of perovskite anodes in air.[23–26]

However, it should be noted that SST15 and SST35 indicate more promising electrical conductivity in comparison to other compounds within a perovskite structure (Fig. 3), especially at temperatures lower that 600°C in air. Moreover, it is widely agreed that a minimum electrical conductivity of 1 S/cm is required for pure SOFC electrode materials.[27] Also, the curves are not linear, signifying that the activation energy is not constant.

Figure 4 shows the relationship between ln (σ) and 1/T. The activation energy is calculated from the slope of ln (σ) and 1/T, in accordance with the following equation:

$$\sigma = \sigma_0 \exp\left(\frac{-Ea}{KT}\right) \quad (3)$$

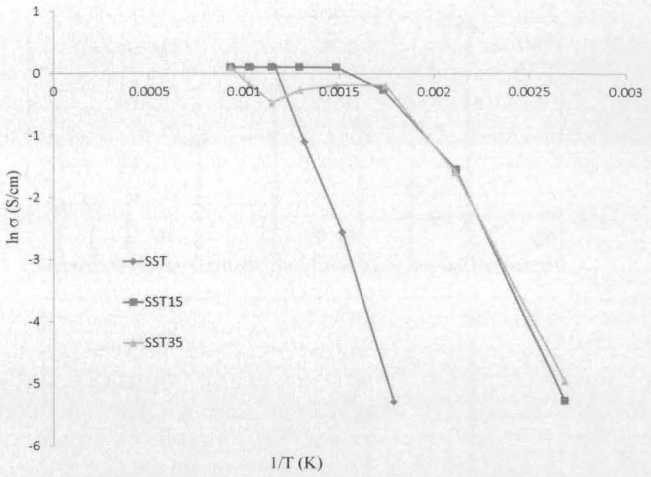

Fig. 4. Relationship between ln (σ) and 1/T of SST samples.

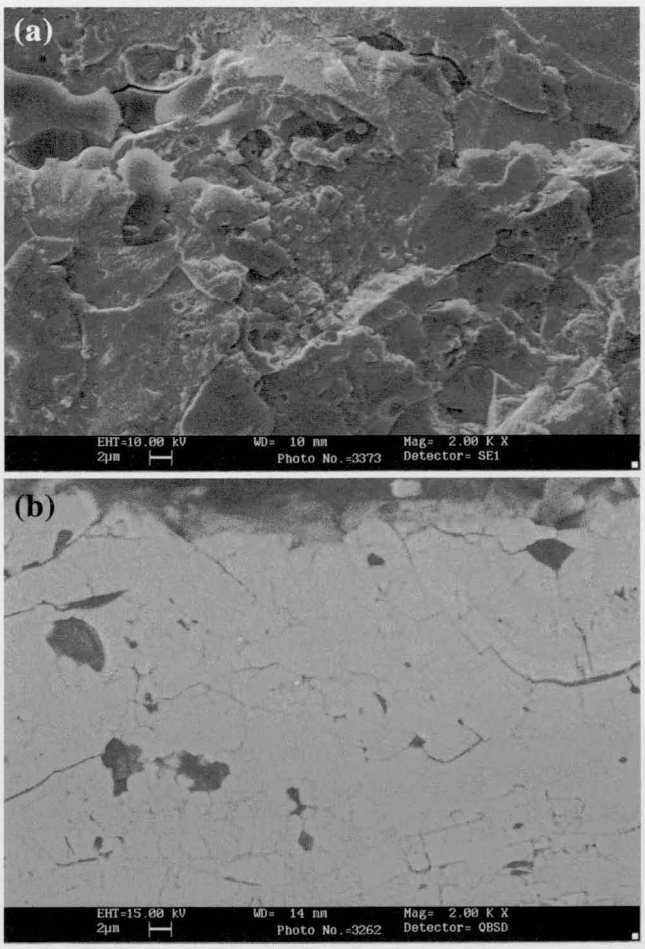

Fig. 5. Scanning electron microscopy (backscattered mode) of SST35: (a) top surface of the coating and (b) polished cross section of the coating.

where σ_0 is the pre-exponential factor, Ea is the activation energy, and K is the Boltzmann constant.[28]

The *Ea* is 58.08 kJ/mol (0.52 eV), 23.33 kJ/mol (0.24 eV), and 20.37 kJ/mol (0.21 eV) for SST, SST15, and SST35, respectively. The results in Fig. 4 show that the activation energy has been reduced, which is consistent with increasing the electrical conductivity of doped samples, as shown in Fig. 2.

SEM Observation

Figure 5a and b show the SEM micrograph of SST35. Figure 5a illustrates a picture of the top surface of the coating showing fully melted particles forming splats. Some splashed particles (known as satellites) are also shown that are the result of high-speed collision of droplets on the surface. These satellites are to some extent responsible for porosity in the coating. Figure 5b shows a cross section of the coating. In this micrograph, pancake-shaped splats and mechanical interlock, which is the result of cohesion between splats, can be seen. The overall results of SEM micrographs indicate that the APS working condition is suitable for this type of powder.

CONCLUSION

The $Sr_{1-x}Sm_xTiO_3$ samples were synthesized and applied to a steel substrate by APS technique. Electrical conductivity measurements show that the addition of rare-earth dopant up to 3.5 M% increases conductivity, giving an electrical conductivity of 1.1 S/cm (the minimum required electrical conductivity for anodes) at lower temperatures. This is in contrast with other perovskite-structure materials currently being used as SOFC anodes and offers an opportunity to develop lower temperature cells.

ACKNOWLEDGEMENT

This work funded through the support of the Iran National Science Foundation (INSF), Vice- Presidency for Science and Technology.

REFERENCES

1. Y. Ma, *Ceria-Based Nanocomposite Electrolyte for Low-Temperature Solid Oxide Fuel Cells* (Royal Institute of Technology: Stockholm, 2009).
2. S. Suthirakun, G. Xiao, S.C. Ammal, F. Chen, H.-C. Zur Loye, and A. Heyden, *J. Power Sources* 245, 875 (2013).
3. X. Li, H. Zhao, N. Xu, X. Zhou, C. Zhang, and N. Chen, *Int. J. Hydrogen Energy* 34, 6407 (2009).
4. C.-X. Li, C.-J. Li, and L.-J. Guo, *Int. J. Hydrogen Energy* 35, 2964 (2009).
5. M. Ni, Z. Shao, and K. Chan, *Energies* 7, 4381 (2014).
6. C. Zuo, M.F. Liu, and M.L. Liu, *Sol-Gel Processing for Conventional and Alternative Energy*, ed. M. Aparicio, A. Jitianu, and L.C. Klein (New York: Springer, 2012),.
7. H. Zhao, F. Gao, X. Li, C. Zhang, and Y. Zhao, *Solid State Ionics* 180, 193 (2009).
8. L. Jiang, G. Liang, J. Han, and Y. Huang, *J. Power Sources* 270, 441 (2014).
9. B. Beyribey, B. Timurkutluk, T.Y. ErtuÄŸrul, Ã.I. Timurkutluk, and M.D. Mat, *Ceram. Int.* 39, 7053 (2013).
10. X. Li, H. Zhao, X. Zhou, N. Xu, Z. Xie, and N. Chen, *Int. J. Hydrogen Energy* 35, 7913 (2010).
11. A.A. Yaremchenko, S.G. PatrÃcio, and J.R. Frade, *J. Power Sources* 245, 557 (2014).
12. D. Neagu and J.T.S. Irvine, *Chem. Mater.* 22, 5042 (2011).
13. B. Beata and K. Bogusław, *Process. Appl. Ceram.* 6, 53 (2012).
14. X. Zhou, N. Yan, K.T. Chuang, and J. Luo, *RSC Adv.* 4, 118 (2014).
15. X. Ma, J. Dai, H. Zhang, J. Roth, T.D. Xiao, and D.E. Reisner, *J. Fuel Cell Sci. Technol.* 2, 190 (2005).
16. M. Cuglietta and O. Kesler, *J. Therm. Spray Technol.* 21, 448 (2012).
17. W.-S. Xia, Y.-Z. Yang, H.-O. Zhang, and G.-L. Wang, *Trans. Nonferrous Met. Soc. China* 19, 1539 (2009).
18. L. Zhang, T. Tosho, N. Okinaka, and T. Akiyama, *Metall. Mater. Trans.* 48, 2088 (2007).
19. V.D. Mote, J.S. Dargad, and B.N. Dole, *Nanosci. Nanoeng.* 1, 116 (2013).
20. J. Cheng, *J. Chil. Chem. Soc.* 57, 969 (2012).
21. S. Ramesh, G. Upender, K.J. Raju, G. Padmaja, S.M. Reddy, and C. Reddy, *J. Mod. Phys.* 4, 859 (2013).
22. Y. Ying (Ph.D. Dissertation, Royal Institute of Technology, Stockholm, 2012).
23. G. Xiao, S. Nuansaeng, L. Zhang, S. Suthirakun, A. Heyden, H.-C.Z. Loye, and F. Chen, *J. Mater. Chem. A* 1, 10546 (2013).
24. B. Mirfakhraei, F. Ramezanipour, S. Paulson, V. Birss, and V. Thangadurai, *Front. Energy Res.* 2, 9 (2014).
25. S. Sengodan, J.S. Yoon, M.Y. Yoon, H.J. Hwang, J. Shin, and G. Kim, *ECS Electrochem. Lett.* 2, F45 (2013).
26. B. Amin, N. Singh, T.M. Tritt, H.N. Alshareef, and U. Schwingenschlogl, *Appl. Phys. Lett.* 103, 031907 (2013).
27. B. Smith (Masters, Bucknell University, Lewisburg, OH, 2010).
28. X.-F. Sun, R.-S. Guo, and J. Li, *Ceram. Int.* 34, 219 (2008).